Evidence for first-order orthorhombic-tetragonal and nearly tricritical tetragonal-cubic antiferrodistortive phase transitions in $Ca_{0.43}Sr_{0.57}TiO_3$

Sanjay Kumar Mishra* and Dhananjai Pandey†
School of Materials Science and Technology, Institute of Technology, Banaras Hindu University, Varanasi-221 005, India
(Received 19 December 2008; published 20 May 2009)

Temperature dependence of the symmetry-adopted strains (secondary order parameter) associated with the antiferrodistortive-phase transitions involving change in space groups from $Pm\bar{3}m$ to $I4/mcm$ and $I4/mcm$ to $Pnma$ in $Ca_{0.57}Sr_{0.43}TiO_3$ have been investigated using powder x-ray diffraction data in the temperature range of 300–950 K. It is argued that the experimentally determined critical exponent $\beta \sim 0.33 \pm 0.03$ in the temperature range $0.70 \leq T \leq 0.98T_c$ for the $I4/mcm$ to $Pm\bar{3}m$ transition is due to a nearly tricritical transition. The $Pnma$ to $I4/mcm$ transition is unambiguously identified as first order.

DOI: 10.1103/PhysRevB.79.174111 PACS number(s): 63.70.+h, 61.50.Ks, 91.60.Hg, 64.60.Kw

I. INTRODUCTION

$SrTiO_3$ and $CaTiO_3$ are well known for their quantum paraelectric behavior.[1,2] The mixed compositions, $Ca_{1-x}Sr_xTiO_3$ (CST), undergo quantum ferroelectric, relaxor ferroelectric, and antiferroelectric transitions with increasing Ca^{2+} content in the $SrTiO_3$ matrix for $1.00 \leq x \leq 0.60$.[3,4] Both the end members (i.e., $SrTiO_3$ and $CaTiO_3$) and the mixed compositions exhibit several antiferrodistortive structural-phase transitions also which are linked with the phonon instabilities at the $R(k=\frac{1}{2},\frac{1}{2},\frac{1}{2})$ and $M(k=\frac{1}{2},\frac{1}{2},0)$ points of the cubic Brillouin zone. The antiferrodistortive-phase transitions induced by R and M point instabilities involve tilting of the oxygen octahedra in the antiphase (−ve tilt) and in-phase (+ve tilt) manners, respectively.[5] Thus, $SrTiO_3$, which has a cubic perovskite structure at room temperature, undergoes an antiphase tilt transition to a tetragonal structure (space-group $I4/mcm$, tilt system $a^0a^0c^-$ in the notation of Glazer[6]) below 105 K.[7] This structure seems to remain stable down to the lowest temperature.[8] It has been argued that the antiferrodistortive phase transition of $SrTiO_3$ is responsible for suppressing the ferroelectric order at low temperatures.[9] The other end member, $CaTiO_3$, has an orthorhombic structure (space-group $Pbnm$; tilt system $a^-a^-c^+$) at room temperature which transforms to a tetragonal structure (space-group $I4/mcm$; tilt system $a^0a^0c^-$) somewhere between 1373–1423 K and finally to the cubic ($Pm\bar{3}m$) perovskite structure above 1523 K.[10] Kennedy *et al.*[11] speculated about the existence of yet another intermediate phase with $Cmcm$ space group (tilt system $a^0b^+c^-$) in between the orthorhombic ($a^-a^-c^+$) and the tetragonal ($a^0a^0c^-$) phases, but this possibility has now been ruled out in a recent work.[12]

The nature of antiferrodistortive-phase transition in $SrTiO_3$ has attracted enormous attention[5] but is still controversial as both asymptotic critical[13] and mean-field[14,15] behaviors have been reported. The situation in $CaTiO_3$ is even more complex as it involves both R and M point instabilities. Going by symmetry arguments, the transition from $Pbnm$ to $I4/mcm$ is expected to be first order, in agreement with the recent observation of a small discontinuous change in the cell parameters at the transition temperature.[12] For the $I4/mcm$ to $Pm3m$ transition, both second-order[10] and tricritical[11] behaviors have been reported. However, most of these conclusions cannot be relied on as they have been drawn on the basis of a very few data points in the stability region of the $I4/mcm$ phase.[10,11,16] Because of the very high temperatures involved, and also limited temperature range of stability ($\sim 125 \pm 25$ K) of the $I4/mcm$ phase, it is rather difficult to settle this issue in pure $CaTiO_3$. 10–20 % substitution of Fe at the Ti site has been shown to lower the transition temperatures, but the stability region of the $I4/mcm$ phase is still low ($\sim 100 \pm 10$ K).[17] We have recently shown[18] that 57% Sr^{2+} substitution at the Ca^{2+} site not only lowers the two-transition temperatures drastically but also enhances the stability field of the $I4/mcm$ phase to ~350 K range. We have exploited this enhanced stability field to capture the variation in the tetragonal cell parameters with temperature more precisely than the earlier workers and to understand the nature of the $Pnma$ to $I4/mcm$ and $I4/mcm$ to $Pm\bar{3}m$ transitions convincingly within the framework of mean-field theories. We have investigated the antiferrodistortive-phase transitions of $Ca_{0.43}Sr_{0.57}TiO_3$ (CST57) using our earlier reported x-ray powder diffraction data[18] in the temperature range of 300–950 K. It is shown that the $Pbnm$ to $I4/mcm$ phase transition in CST57 is first order as confirmed by discontinuous change in the symmetry-adopted strain (secondary order parameter). We also show that the $I4/mcm$ to $Pm\bar{3}m$ transition may be close to tricritical with an effective exponent $\beta \approx 0.33 \pm 0.03$. The entire analysis has been carried out using 2-4-6 Landau potential expansion considering primary and secondary order parameter terms as also the coupling terms.[16] The value of the coefficient of the fourth-order term in the Landau expansion is shown to be nearly zero as expected for a tricritical transition. We believe that the strain produced by the distortion of the lattice due to the antiferrodistortive transitions in CST57 is large enough to promote long-range interactions and hence the mean-field behavior.

II. EXPERIMENTAL

$Ca_{0.57}Sr_{0.43}TiO_3$ powder was prepared by the solid-state ceramic route at 1423 K for 6 h using 99% pure $SrCO_3$, $CaCO_3$, and TiO_2. The powders were sintered at 1573 K. The high-temperature x-ray diffraction studies were carried out using a 12 kW rotating Cu anode-based Rigaku powder diffractometer (RINT 2000/PC series) fitted with a Rigaku high-

temperature attachment and a curved-crystal monochromator. The temperature was stable within ±1 K during these measurements. Rietveld refinement was carried out using FULLPROF package.[19] Pseudo-Voigt function was used to model the peak profiles, while background was fitted to sixth-order polynomial. The occupancy parameters of the atoms were fixed at the nominal composition, whereas other parameters, i.e., lattice parameters, positional coordinates, and isotropic thermal parameters, were refined.

III. PRINCIPLE OF ANALYSIS

Carpenter *et al.*[16] recently proposed the following Landau free-energy expression for antiferrodistortive-phase transitions in cubic perovskites driven by the R_4^+ and M_3^+ point instabilities with component primary order parameters q_1, q_2, q_3, q_4, q_5, and q_6, respectively, which are coupled to the symmetry-adapted strains e_a, e_o and e_t (secondary order parameters);

$$
\begin{aligned}
G = {} & \frac{1}{2}a_1(T-T_{c1})(q_1^2+q_2^2+q_3^2) + \frac{1}{2}a_2(T-T_{c2})(q_4^2+q_5^2+q_6^2) + \frac{1}{4}b_1(q_1^2+q_2^2+q_3^2)^2 + \frac{1}{4}b_1'(q_1^4+q_2^4+q_3^4) + \frac{1}{4}b_2(q_4^2+q_5^2+q_6^2)^2 \\
& + \frac{1}{4}b_2'(q_4^4+q_5^4+q_6^4) + \frac{1}{6}c_1(q_1^2+q_2^2+q_3^2)^3 + \frac{1}{6}c_{1_1}'(q_1q_2q_3)^2 + \frac{1}{6}c_1''(q_1^2+q_2^2+q_3^2)(q_1^4+q_2^4+q_3^4) + \frac{1}{6}c_2(q_4^2+q_5^2+q_6^2)^3 \\
& + \frac{1}{6}c_2'(q_4q_5q_6)^2 + \frac{1}{6}c_2''(q_4^2+q_5^2+q_6^2)(q_4^4+q_5^4+q_6^4) + \lambda_q(q_1^2+q_2^2+q_3^2)(q_4^2+q_5^2+q_6^2) + \lambda_q'(q_1^2q_4^2+q_2^2q_5^2+q_3^2q_6^2) \\
& + \lambda_1 e_a(q_1^2+q_2^2+q_3^2) + \lambda_2 e_a(q_4^2+q_5^2+q_6^2) + \lambda_3[\sqrt{3}e_0(q_2^2-q_3^2) + e_t(2q_1^2-q_2^2-q_3^2)] + \lambda_4[\sqrt{3}e_0(q_5^2-q_6^2) + e_t(2q_4^2-q_5^2-q_6^2)] \\
& + \lambda_5(e_4q_4q_6 + e_5q_4q_5 + e_6q_5q_6) + \lambda_6(q_1^2+q_2^2+q_3^2)(e_4^2+e_5^2+e_6^2) + \lambda_7(q_1^2e_6^2+q_2^2e_4^2+q_3^2e_5^2) + \frac{1}{4}(C_{11}^0-C_{12}^0)(e_o^2+e_t^2) \\
& + \frac{1}{6}(C_{11}^0+2C_{12}^0)e_a^2 + \frac{1}{2}C_{44}^0(e_4^2+e_5^2+e_6^2). \qquad (1)
\end{aligned}
$$

a_1, a_2, b_1, b_1', b_2, b_2', c_1, c_{1_1}', c_1'', c_2, c_2', and c_2'' are the normal Landau coefficients. T_{c1} and T_{c2} are the critical temperatures corresponding to the in-phase and antiphase tilt transitions. λ_1 to λ_7 are the coupling coefficients between the primary and secondary order parameters. C_{11}^0, C_{12}^0, and C_{44}^0 are the bare elastic constants. e_4, e_5, and e_6 are the shear-strain components while e_1, e_2, and e_3 are the normal-strain components along the [100], [010], and [001] directions of the elementary pseudocubic perovskite cell. The symmetry-adapted strains, e_a, e_o and e_{tz} are linear combinations of the normal strain components e_1, e_2, and e_3 as follows:

$$e_a = (e_1 + e_2 + e_3), \qquad (2)$$

$$e_o = (e_1 - e_2), \qquad (3)$$

$$e_{tz} = \frac{1}{\sqrt{3}}(2e_3 - e_1 - e_2), \qquad (4)$$

where the subscript, z, in Eq. (4) signifies that the tetragonal axis is parallel to the reference z-axis, i.e., [001] of the pseudocubic perovskite cell.[16] For the $I4/mcm$ structure, the only nonzero-order parameter component is q_4 whereas the spontaneous strain components are given by

$$e_1 = e_2 = \frac{\frac{a}{\sqrt{2}} - a_o}{a_o}, \quad e_3 = \frac{\frac{c}{2} - a_o}{a_o}, \qquad (5)$$

where a_o is the reference cell parameter of the cubic perovskite structure extrapolated into the tetragonal-stability field, and a and c are the equivalent perovskite cell parameters of the tetragonal $I4/mcm$ structure. The tetragonal cell parameters (A_t, B_t, C_t) are related to a and c as $A_t = B_t \approx \sqrt{2}\,a$, whereas $C_t \approx 2c$. The primary-order parameter (q_4) for the $I4/mcm$ structure is related to the secondary order parameters in the following manner:[16]

$$e_a = -\frac{\lambda_2 q_4^2}{\frac{1}{3}(C_{11}^o + 2C_{12}^0)}, \qquad (6)$$

$$e_{tz} = -\frac{2\lambda_4 q_4^2}{\frac{1}{2}(C_{11}^0 - C_{12}^0)}, \qquad (7)$$

$$e_o = e_4 = e_5 = e_6 = 0. \qquad (8)$$

It is evident from Eqs. (6) and (7) that from a study of the temperature dependence of the symmetry-adopted strains e_{tz} and e_a, one can obtain information about the temperature variation of the primary-order parameter (q_4) of the tetragonal phase.

For the orthorhombic *Pnma* structure (which is equivalent to *Pbnm* with a different setting of axes), $q_1=q_3=q_5=0$ but $q_2\neq 0$ and $q_4=q_6\neq 0$. The individual strain components for the orthorhombic phase are given by

$$e_1 = \frac{\frac{b}{2} - a_o}{a_o}, \tag{9}$$

$$e_2 + e_3 = \frac{\frac{a}{\sqrt{2}} - a_o}{a_o} + \frac{\frac{c}{\sqrt{2}} - a_o}{a_o}, \tag{10}$$

$$|e_4| = \left| \frac{\frac{a}{\sqrt{2}} - a_o}{a_o} - \frac{\frac{c}{\sqrt{2}} - a_o}{a_o} \right|, \tag{11}$$

where a, b, and c are the equivalent perovskite cell parameters related with the A_o, B_o, and C_o parameters of the orthorhombic *Pnma* structure as $A_o \approx \sqrt{2}\ a$ and $B_O \approx 2b$ $B_o \approx \sqrt{2}c$. The symmetry adapted secondary order parameters are related to q_2 and q_4 according to Ref. 16,

$$e_a = -\frac{(\lambda_1 q_2^2 + 2\lambda_2 q_4^2)}{\frac{1}{3}(C_{11}^o + 2C_{12}^0)}, \tag{12}$$

$$e_{tx} = -\frac{2(\lambda_3 q_2^2 - \lambda_4 q_4^2)}{\frac{1}{2}(C_{11}^0 - C_{12}^0)}, \tag{13}$$

$$e_4 \approx -\frac{\lambda_5}{c_{44}^0} q_4^2, \tag{14}$$

$$e_o = e_5 = e_6 = 0. \tag{15}$$

An additional term $(\lambda_6+\lambda_7)e_4^2 q_2^2$ in Eq. (14) has been ignored since its contribution is expected to be very small.[16]

In addition to the secondary order parameters, we have also analyzed the temperature dependence of the tilt angle (which is the primary-order parameter) to evaluate the coefficients of the second-, fourth-, and sixth-order terms in the Landau "2:4:6" potential.

IV. RESULTS AND DISCUSSIONS

Figure 1 depicts the temperature variation of equivalent elementary perovskite cell parameters in the *Pbnm* setting, as obtained by Rietveld analysis of the powder-diffraction data at various temperatures, published earlier.[18] For calculating the symmetry-adapted strains at various temperatures

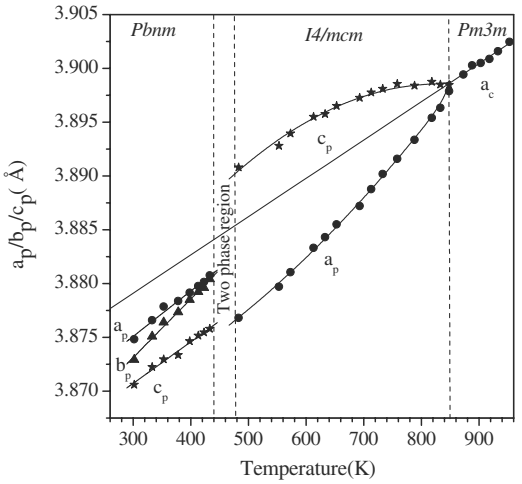

FIG. 1. The variation in equivalent elementary perovskite cell parameters (a_p, b_p, c_p) of $Ca_{0.43}Sr_{0.57}TiO_3$ with temperature (after Ref. 18).

in the tetragonal and orthorhombic-phase fields, we extrapolated the cubic-cell parameter up to room temperature. The best linear fit to the cubic lattice-parameter values in the temperature range of 850–950 is described by a (Å) $=3.861\ 27+0.000\ 04$ T (K). The fit and its extrapolation below 850 K are shown with a straight line in Fig. 1. The spontaneous strains, calculated according to Eqs. (5) and (9)–(11) for each structure were used to calculate the values of the symmetry-adapted strains e_a, e_{tx}, and e_4 for the orthorhombic phase and e_a and e_{tz} for the tetragonal phase, as per the relationships given by Eqs. (12)–(15), (6), and (7), respectively. The variations in these symmetry-adapted strains are shown in Fig. 2(a). Both e_4 and e_{tx} change discontinuously and become e_{tz} of the tetragonal phase at the orthorhombic to tetragonal-phase transition temperature of 463 K. The volume strain e_a, on the other hand, varies smoothly across the transition temperature. The discontinuous change in the symmetry-adopted strains e_4 and e_{tx} confirms first-order nature of the *Pnma* to $I4/mcm$ transition, as expected from symmetry considerations also. The e_{tz} of the tetragonal phase decreases in a nonlinear fashion upon approaching the tetragonal to cubic transition temperature. The variation in e_{tz}^2 [which is proportional to the fourth power of primary-order

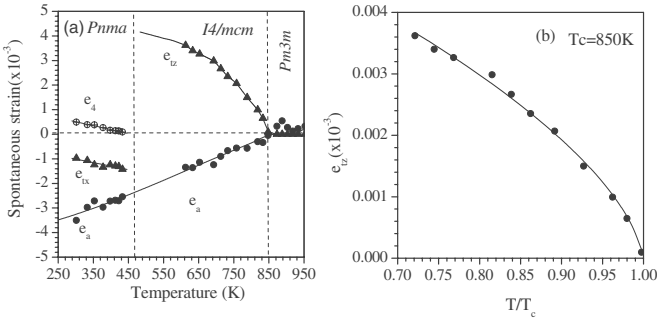

FIG. 2. (a) The variation in symmetry-adopted strains of $Ca_{0.43}Sr_{0.57}TiO_3$ with temperature. (b) The variation in e_{tz} with T/T_c. The dots represent experimental values, while the continuous line corresponds to the least-squares fit for $e_{tz} \sim (T_c\text{-}T)^{2\beta}$.

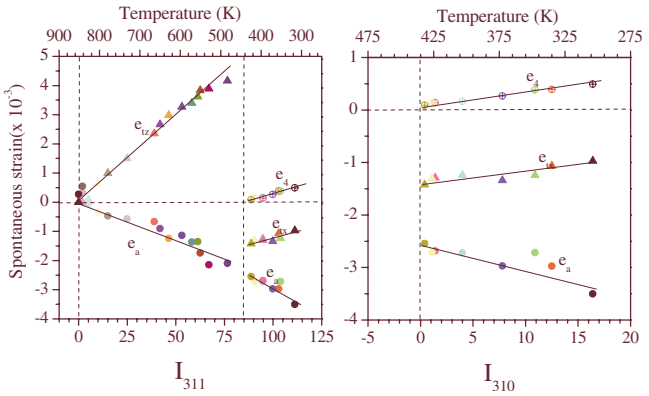

FIG. 3. (Color online) Symmetry-adopted strains plotted against the integrated intensities of the 311 and 310 [the indices are with respect to a doubled perovskite cell (Ref. 6) superlattice peaks associated with antiferrodistortive-phase transitions driven by $R(q=\frac{1}{2},\frac{1}{2},\frac{1}{2})$- and $M(q=\frac{1}{2},\frac{1}{2},0)$-point phonon instabilities. For clarity temperature axis is shown on the top of the panel. Different color symbols correspond to different temperatures.

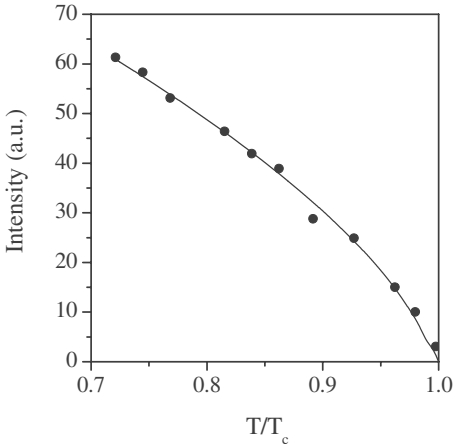

FIG. 4. The variation in the intensity of the 311 superlattice peak with temperature. The dots represent experimental values, while the continuous line corresponds to the least-squares fit for $I_{311} \sim (T_c\text{-}T)^{2\beta}$.

parameter (q_4) as per Eq. (6)] with temperature shows a nearly linear dependence indicating tricritical behavior corresponding to $q \sim (T-T_c)^{1/4}$. However, a more rigorous least-squares fit to the data in the temperature-range of $0.70-0.98T_c$ in Fig. 2(a) using the expression $e_{tz} \sim (T_c-T)^{2\beta}$ gives an effective exponent $\beta=0.31\pm0.02$ with $T_c=850$ K, which is shown in Fig. 2(b).

We have also determined the effective exponent using the intensity of the superlattice reflections. As pointed out by Glazer,[6] the intensities of the odd-odd-odd (ooo)- and odd-odd-even (ooe)-type reflections are related to the amplitude of the antiphase and in-phase tiltings of the TiO_6 octahedra about the [001] pseudocubic axes, corresponding to the $R(k=\frac{1}{2},\frac{1}{2},\frac{1}{2})$- and $M(k=\frac{1}{2},\frac{1}{2},0)$-point phonon instabilities of the cubic Brilloun zone. The general relation between the order parameter (q) and the intensity (I) of these superlattice reflections is $I \alpha q^2$. Since the secondary order parameters are also proportional to q^2 [see Eqs. (6) and (11)], one expects linear relationship between the secondary order parameters shown in Fig. 2 and the intensities of the corresponding superlattice reflections. Figures 3(a) and 3(b) depict the plot of secondary order parameters vs integrated intensity of the 311 and 310 superlattice reflections at each temperature. The nearly linear relationship confirms the consistency of the secondary order parameter and the intensity data. Figure 4 depicts the temperature dependence of the integrated intensity of the 311 superlattice reflection as a function of temperature. The solid line gives the least-squares fit for the power law $I \propto (T_c-T)^{2\beta}$ for which a critical exponent of $\beta \approx 0.33\pm0.03$ was determined for $T_c=850$ K. This β value is in agreement with the value obtained from the symmetry-adopted strain within the standard deviations.

It is evident from the foregoing that the effective exponent (β) obtained by using both the symmetry-adapted strains and the intensity of the superlattice reflections lies in the range from 0.31 to 0.33 ± 0.03 for the temperature interval to $0.70-0.98T_c$. Attempts to fit a limited set of data points in a narrower temperature range did not alter the value of exponent (β). $\beta \sim 1/3$ has been reported by Muller and Behinger[13] for $I4/mcm$ to $Pm\bar{3}m$ and $R\bar{3}c$ to $Pm\bar{3}m$ transitions in $SrTiO_3$ and $LaAlO_3$ using electron paramagnetic resonance (EPR) measurements in a narrow temperature range of about $0.95T_c<T<T_c$. This observation was interpreted as failure of Landau theory in the critical region close to T_c where critical fluctuations are expected to play an important role. For $T<0.95T_c$, mean-field exponent $\beta=0.50$ was observed. In our case the linear dependence of e_{tz} and I_{311} is observed up to ~0.80 and $\sim0.85T_c$, respectively, [see Figs. 2(b) and 4] from the higher-temperature side. One may be tempted to treat this as a signature of second-order transition with $\beta=0.50$ for $T<0.85$ T_c and $\beta \sim 0.33\pm0.03$ as departure from the mean-field behavior for $T>0.85$. However, the fits for e_{tz} vs temperature and I_{311} vs temperature in the ranges $0.70<T\leq0.98T_c$ and $0.85<T\leq0.98T_c$, respectively, yield the same value of the exponent β. This suggests that the exponent $\beta \sim 0.33\pm0.03$ is valid in the entire temperature range; i.e., $0.70\leq T\leq0.98T_c$.

In recent years, Salje and co-workers[14,20] argued for $SrTiO_3$ that non-mean-field exponents, such as $\beta \approx 0.35\pm0.02$ (which is close to 1/3 obtained by us), can be rationalized in terms of Landau 2:4:6 potential,

$$G = Aq^2 + Bq^4 + Cq^6, \tag{16}$$

where

$$A = A_o(T - T_c)$$

For a 2:4 Landau potential ($c=0$), the order parameter varies as $q \propto (T_c-T)^{1/2}$ and hence $\beta=1/2$. For 2:6 potential ($B=0$), q varies as $q \propto (T_c-T)^{1/4}$ (i.e., $\beta=1/4$) corresponding to a tricritical transition. However, if B is very small but nonzero, the effective exponent (β) in $q \propto (T_c-T)^{\beta}$ will be between 0.5 and 0.25. In our case, the fact that $\beta \sim 1/3$ is observed for temperatures as low as $0.7T_c$ and as high as $0.98T_c$ suggests a mean-field behavior. Our results also suggest that the asymptotic critical limit lies in the range $0.98T_c<T\leq T_c$ for CST57. We believe that the large spontaneous strain associ-

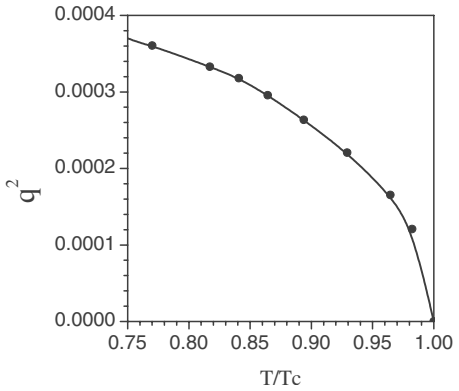

FIG. 5. Variation in q^2 with T/T_c. The dots represent experimental values, while the continuous line corresponds to the calculation predicted by 2:4:6 Landau potential.

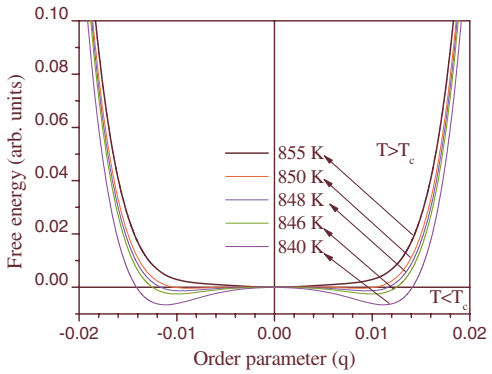

FIG. 6. (Color online) Variation in free energy with order parameter (q) at various temperatures (black: $T=855$ K; red: $T=850$ K; blue: $T=848$ K; purple: $T=846$ K; and violet: $T=840$ K) predicted by 2:4:6 Landau potential.

ated with the primary-order parameter fluctuations induces long-range strain interactions leading to mean-field behavior over such an extended temperature range.

The master expression for the free energy given by Eq. (1) reduces to the form given by Eq. (16) after appropriate renormalization of the coefficients in the former due to elastic energy and coupling terms. In order to determine the coefficients A, B, and C of Eq. (16), we calculated the tilt angles (which is the primary-order parameter) from the Rietveld-refined positional coordinates of atoms at various temperatures. The variation in the square of tilt angle with temperature, associated with the cubic- to tetragonal-phase transition, is shown in Fig. 5. We fitted Eq. (16) to the temperature variation of the square of the primary order parameter (q_4) shown in Fig. 5 and obtained the following values of $A=(4.815\pm0.005)\times10^{32}$, $B=(-2.0905\pm0.0003)\times10^{37}$, and $C=(2.297\ 28\pm0.000\ 07)\times10^{41}$. It is evident that B is negative suggesting a first-order-phase transition. However, its value is negligibly small as compared to C suggesting that the situation may be close to tricritical. The variation in the free energy with order parameter (q_4) as obtained using these values of A, B, and C is shown in Fig. 6. It is evident from this figure that the free-energy curves at $T=T_c$ have a broad, flat-bottom nature characteristic of a second-order/tricritical transition. There is no signature of the coexistence of the cubic and tetragonal phases at T_c in Fig. 6 in terms of the presence of three triply degenerate minima, one for $q=0$ and two for $\pm q$, characteristic of a first-order phase transition. Further, there is no signature of any local minimum or an inflection point in the free-energy curve just above T_c. The two minima corresponding to the equilibrium phase appear at $\pm q$ just below T_c. All these observations clearly show that the negative value of B obtained by our fits is too low to make the transition first order, and as a result the situation becomes close to a tricritical behavior with $C \gg B$. In $SrTiO_3$, both near-tricritical[14] and second-order[15] transitions have been reported. Salje and co-workers[14] argued that the cubic to tetragonal transition is close to tricritical with an effective exponent $\beta \approx 0.35\pm0.02$, which is close to the exponent for CST57 but with one significant difference. In $SrTiO_3$, B is positive and is not negligibly small as compared to C whereas it is negative and negligibly small for CST57.

What could be the origin of vanishingly small value of B in Eq. (6)? We recall that the cubic to tetragonal transition requires antiphase rotation of octahedra about the pseudocubic ⟨100⟩ direction. The second transition (tetragonal to orthorhombic) requires additional in-phase rotation of the octahedra about the pseudocubic ⟨110⟩ direction. In the cubic phase, both the instabilities involving antiphase and in-phase octahedral rotations are present although the corresponding phonon modes freeze one after the other at two different temperatures (T_{c1} and T_{c2}) leading to the two-phase transitions. It is therefore quite likely that the two order parameters (q_4 and q_2) and the two modes could be coupled in the cubic phase itself. In addition, the tetragonal to orthorhombic transition leads to very pronounced distortion of the lattice [see Figs. 1 and 2(a)]. This would mean significant contribution of the elastic energy [last few terms of Eq. (1)] and also the strain-order parameter (e-q^2) coupling terms of Eq. (1). Both these terms would renormalize the coefficients of the fourth-order terms in q in Eq. (1). The coefficient B in Eq. (16) is thus the renormalized coefficient. Depending on the strength of the e-q^2 coupling, the sign of B can be positive or negative leading to a second-order or a first-order phase transition. This coupling is apparently very strong for tetragonal to orthorhombic transition making it first order. This coupling can influence the nature of the cubic to tetragonal-phase transition also. Since the tetragonal to orthorhombic transition (order-parameter q_2) is first order, it is expected that the coefficient B in Eq. (16) would have positive contribution from q_4 and negative contribution from q_2. When the negative contribution outweighs the positive one, the low-temperature transition at T_{c2} becomes first order. However, for the higher-temperature transition (i.e., cubic to tetragonal), it appears that the two contributions to B are nearly equal leading to vanishingly small value of B. This is the most likely explanation for the tricritical behavior of the cubic to tetragonal-phase transition.

To summarize, we have studied the temperature dependence of secondary order parameters for cubic $Pm\bar{3}m$ to tetragonal ($I4/mcm$) and tetragonal ($I4/mcm$) to orthorhombic ($Pnma$) antiferrodistortive-phase transitions in $Ca_{0.43}Sr_{0.57}TiO_3$(CST57). The discontinuous jump and con-

tinuous variation in the secondary order parameter for the tetragonal to orthorhombic and cubic to tetragonal transitions suggest first- and second-order characters, respectively. The critical exponent (β) for the cubic to tetragonal-phase transition, as obtained from the temperature variation of second ary and primary-order parameters, corresponds to a value of $\beta \approx \frac{1}{3}$. It is argued that this exponent is due to a nearly tricritical transition. The free-energy calculations support this picture.

One of us (D.P.) acknowledges a useful discussion with T. V. Ramakrishnan.

*Present address: Solid State Physics Division, Bhabha Atomic Research Centre, Tombay, Mumbai 400085, India.
†dpandey_bhu@yahoo.co.in

[1] K. A. Muller and H. Burkard, Phys. Rev. B **19**, 3593 (1979).
[2] I. S. Kim, M. Itoh, and T. Nakamura, J. Solid State Chem. **101**, 77 (1992).
[3] J. G. Bednorz and K. A. Muller, Phys. Rev. Lett. **52**, 2289 (1984).
[4] R. Ranjan, D. Pandey, and N. P. Lalla, Phys. Rev. Lett. **84**, 3726 (2000); R. Ranjan, and D. Pandey, J. Phys.: Condens. Matter **13**, 4239 (2001); **13**, 4251 (2001).
[5] A. D. Bruce and R. A. Cowely, Adv. Phys. **29**, 219 (1980).
[6] A. M. Glazer, Acta Crystallogr. **B28**, 3384 (1972); **31**, 756 (1975).
[7] H. Unoki and T. Sakudo, J. Phys. Soc. Jpn. **23**, 546 (1967); G. Shirane and Y. Yamada, Phys. Rev. **177**, 858 (1969).
[8] J. M. Kiat and T. Roisnel, J. Phys.: Condens. Matter **8**, 3471 (1996).
[9] W. Zhong and D. Vanderbilt, Phys. Rev. Lett. **74**, 2587 (1995).
[10] S. A. T. Redfern, J. Phys.: Condens. Matter **8**, 8267 (1996).
[11] B. J. Kennedy, C. J. Howard, and B. C. Chakoumakos, J. Phys.: Condens. Matter **11**, 1479 (1999).
[12] R. Ali and M. Yashima, J. Solid State Chem. **178**, 2867 (2005).
[13] K. A. Muller and W. Berlinger, Phys. Rev. Lett. **26**, 13 (1971).
[14] S. A. Hayward and E. K. H. Salje, Phase Transitions **68**, 501 (1999); M. C. Gallardo, J. Jimenez, J. del Cerro, and E. H. K. Salje, J. Phys.: Condens. Matter **8**, 83 (1996); E. H. K. Salje, M. C. Gallardo, J. Jimenez, F. J. Romero, and J. del. Cerro, *ibid.* **10**, 5535 (1998).
[15] M. A. Geday and A. M. Glazer, J. Phys.: Condens. Matter **16**, 3303 (2004).
[16] M. A. Carpenter, C. J. Howard, K. S. Knight, and Z. Zhang, J. Phys.: Condens. Matter **18**, 10725 (2006).
[17] A. I. Becerro, S. A. T. Redfern, M. A. Carpenter, K. S. Knight, and F. Seifert, J. Solid State Chem. **167**, 459 (2002).
[18] S. K. Mishra, R. Ranjan, D. Pandey, R. Ouillan, J.-P. Pinan-Lucarre, P. Ranson, and Ph. Pruzan, J. Phys.: Condens. Matter **18**, 1899 (2006).
[19] J. Rodriguez-Carvajal, Physica B **192**, 55 (1993).
[20] E. K. H. Salje, J. Mc Jimenz Gallardo, F. J. Romero, and J. del Cerro, J. Phys.: Condens. Matter **10**, 5535 (1998).